frontiers in Energy Research

BRIEF RESEARCH REPORT
published: 30 November 2021
doi: 10.3389/fenrg.2021.770342

Optimal Placement and Sizing of Distributed Generators Based on Multiobjective Particle Swarm Optimization

Deyu Yang[1], Junqing Jia[1], Wenli Wu[1], Wenchao Cai[1], Dong An[1], Ke Luo[2] and Bo Yang[3]*

[1]Inner Mongolia Power Research Institute, Huhhot, China, [2]School of Information and Electrical Engineering, Shandong Jianzhu University, Jinan, China, [3]Faculty of Electric Power Engineering, Kunming University of Science and Technology, Kunming, China

To solve the problems of environmental pollution and energy consumption, the development of renewable energy sources becomes the top priority of current energy transformation. Therefore, distributed power generation has received extensive attention from engineers and researchers. However, the output of distributed generation (DG) is generally random and intermittent, which will cause various degrees of impact on the safe and stable operation of power system when connected to different locations, different capacities, and different types of power grids. Thus, the impact of sizing, type, and location needs to be carefully considered when choosing the optimal DG connection scheme to ensure the overall operation safety, stability, reliability, and efficiency of power grid. This work proposes a distinctive objective function that comprehensively considers power loss, voltage profile, pollution emissions, and DG costs, which is then solved by the multiobjective particle swarm optimization (MOPSO). Finally, the effectiveness and feasibility of the proposed algorithm are verified based on the IEEE 33-bus and 69-bus distribution network.

Keywords: distribution network, distributed generation, optimal sizing and placement, multiobjective particle swarm optimization, metaheuistic optimization

OPEN ACCESS

Edited by:
Bin Zhou,
Hunan University, China

Reviewed by:
Yang Li,
Northeast Electric Power University, China
Xiaoshun Zhang,
Shantou University, China

****Correspondence:***
Ke Luo
Ke.Luo96@outlook.com

Specialty section:
This article was submitted to Process and Energy Systems Engineering, a section of the journal Frontiers in Energy Research

Received: *03 September 2021*
Accepted: *20 September 2021*
Published: *30 November 2021*

Citation:
Yang D, Jia J, Wu W, Cai W, An D, Luo K and Yang B (2021) Optimal Placement and Sizing of Distributed Generators Based on Multiobjective Particle Swarm Optimization. Front. Energy Res. 9:770342. doi: 10.3389/fenrg.2021.770342

INTRODUCTION

With the rapid development of the world's electric power industry, the total amount of social electricity consumption has risen sharply over the last decade (Yang et al., 2016; Yang et al., 2017; Zhang et al., 2021). Under the traditional grid framework, the power sector mainly builds large centralized power sources such as nuclear power stations, large hydropower stations, and coal-fired power stations and then expands into a large-scale power system (Yang et al., 2019a; Yang et al., 2019b; Yan, 2020). However, its disadvantages are also increasingly prominent (Li et al., 2020; Xi et al., 2020), in particular, highly centralized power supply is gradually difficult to meet the flexibility requirements of power grid operation, and the failure of important power supply nodes seriously affects the overall reliability of power grid's power supply. Moreover, long-distance transmission is also under serious power loss and security problems (Mehleri et al., 2012; Wang et al., 2014; Yang et al., 2018).

To overcome the negative impact of the aforementioned problems, the concept of distributed generation (DG) was put forward in the 1980s (GopiyaNaik et al., 2013; Yang et al., 2015). DG has an

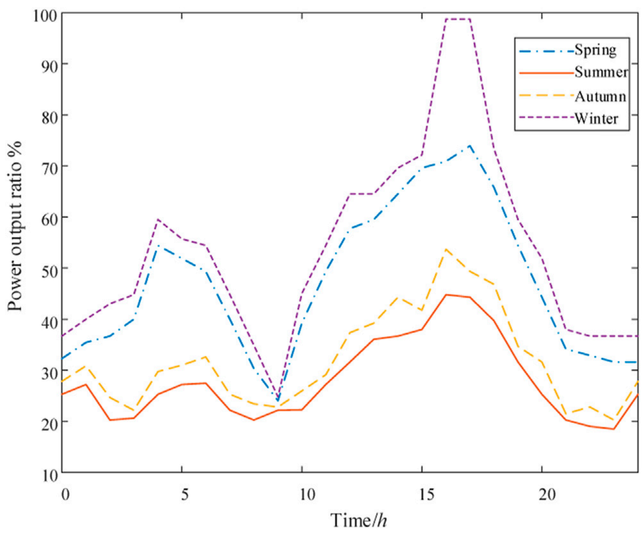

FIGURE 1 | Annual output curve of wind turbine.

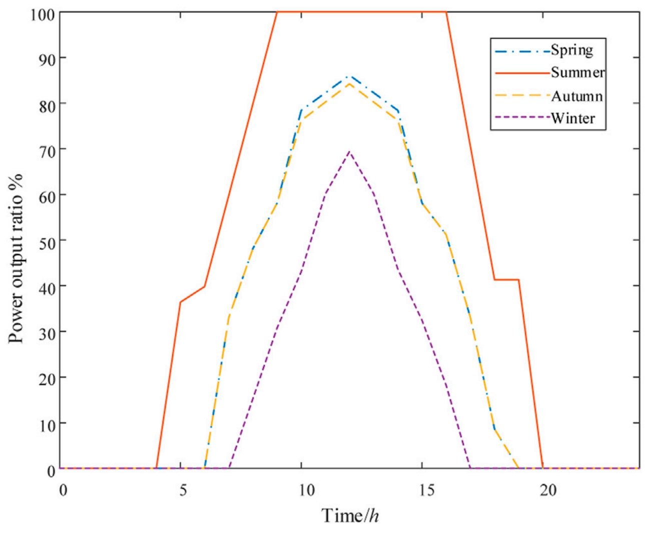

FIGURE 2 | Annual output curve of PV system.

extremely important influence on the planning and operation of the distribution network (Sara et al., 2020; Yang et al., 2020; Ali and Mohammad, 2021). Also, proper access of DG in distribution network can effectively enhance the power quality, reduce the active power loss, improve the voltage distribution, and boost the overall economy and flexibility of the power network operation (Abdurrahman et al., 2020; Bikash et al., 2020; Suresh and Edward, 2020). As the end of power network, the stability and efficiency of distribution network directly affect its overall efficiency (Surajit and Parimal, 2018; Bikash et al., 2019). Therefore, the location and sizing of distributed power generation have become an important research content of power grid planning.

The problem of location and sizing of DG is to optimize its installation point and sizing to maximize the benefits under the constraints of satisfying the given investment and system operation (Kumar et al., 2019; Nagaballi and Kale, 2020). With the increasing requirements for power system reliable operation, the problem of DG location and constant sizing has developed from a single-objective problem that only considers the minimum network loss to a multiobjective optimization problem that comprehensively considers voltage quality, current quality, and environmental factors. Quadratic programming method, genetic algorithm, and other methods have been applied to solve such multiobjective location and constant volume problem. These methods all need to set weights to transform the multiobjective problem into a single-objective problem for proper solutions (Murty and Kumar, 2015); however, these weights are often difficult to determine in actual operation.

Besides, the solution of a large number of planning models is relatively complicated, while the selection of the algorithm directly affects the choice of planning schemes (Aman et al., 2014; Nezhadpashaki et al., 2020; Zeng and Shu, 2020). At present, the solving algorithms mainly include mathematical optimization and metaheuristic algorithm (Doagou-Mojarrad et al., 2013; Satish et al., 2013; Sultana et al., 2016). However, mathematical optimization algorithm owns relatively low computational efficiency and is only suitable for small-scale distribution networks. Thus, metaheuristic algorithm has received much attention and application in recent years (Aman et al., 2012; Pabu and Singh, 2016; Iqbal et al., 2018). Literature (Chandrasekhar and Sydulu, 2012) adopts genetic algorithm (GA) to optimize the new load nodes for expansion plan of distribution network, and then simulated annealing algorithm is utilized to optimize the generated single plan, which considerably reduces the load size of DG connected to the distribution network and the influence of power flow of the distribution network. Literature (Aman et al., 2013) proposes an improved particle swarm optimization algorithm based on hybrid

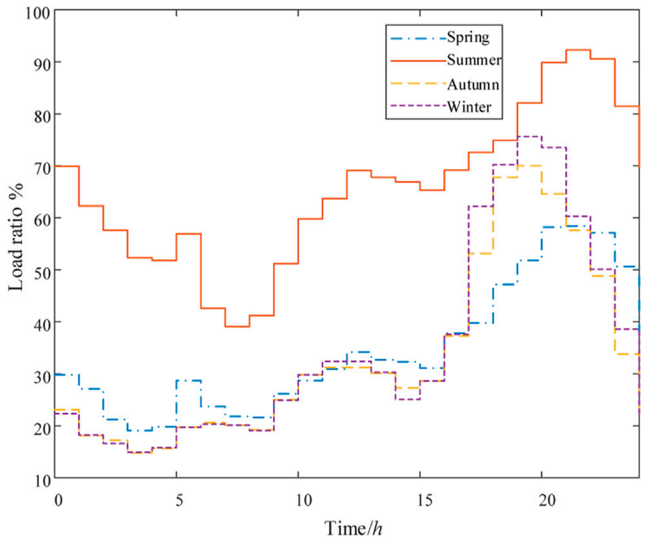

FIGURE 3 | Annual load curve of residents.

simulated annealing method to optimize the location and sizing of distributed power sources. However, the convergence speed of the aforementioned algorithms is relatively slow, and the result is prone to local optimal solutions.

Therefore, an objective function comprehensively considering power losses, voltage profile, pollution emission, and DG cost is proposed in this work, and MOPSO is utilized to solve it. Finally, the proposed method is validated via an IEEE 33-bus and 69-bus distribution network to verify its effectiveness. Then, the Pareto front result is given.

The remaining of this paper is organized as follows: *Mathematical Optimization Model of DG Planning* develops the objective function. In *Multiobjective Particle Swarm Optimization Algorithm*, multiobjective particle swarm optimization (MOPSO) is described. Comprehensive case studies are undertaken in *Case Studies*. At last, *Conclusion* summarizes the main contributions of the paper.

MATHEMATICAL OPTIMIZATION MODEL OF DG PLANNING

Load and DG Power Output Timing Model

Wind Turbine Output Timing Model

The output power of wind turbine mainly depends on wind speed, which can be expressed by the following piecewise function (Velasquez et al., 2016):

$$P(v) = \begin{cases} 0 & (v \le v_{\mathrm{ci}}\, \partial v \ge v_{\mathrm{co}}) \\ P_{\mathrm{r}} \dfrac{v - v_{\mathrm{ci}}}{v_{\mathrm{R}} - v_{\mathrm{ci}}} & (v_{\mathrm{ci}} \le v \le v_{\mathrm{R}}) \\ P_{\mathrm{r}} & (v_{\mathrm{R}} \le v \le v_{\mathrm{co}}) \end{cases}, \tag{1}$$

where $P(v)$ is the power output of the wind turbine; v_{ci} denotes the entry wind speed; v_{co} is the cut-out wind speed; v_{R} means rated wind speed; P_{r} represents the rated output power. The wind turbine output curve is modeled according to the mean seasonal wind speed, and the output curve is shown in **Figure 1** (Sara et al., 2020).

Photovoltaic System Output Timing Model

The output power P_{PV} of the photovoltaic (PV) system can be approximated by (Velasquez et al., 2016)

$$P_{\mathrm{PV}} = P_{\mathrm{stc}} \frac{I_{\mathrm{r,t}}}{I_{\mathrm{stc}}} \left[1 + \alpha_{\mathrm{T}} (T_{\mathrm{t}} - T_{\mathrm{stc}})\right], \tag{2}$$

where P_{stc} means the output power of the PV system when the solar radiation intensity $I_{\mathrm{stc}} = 1000\mathrm{W/m^2}$ and the temperature $T_{\mathrm{stc}} = 25°\mathrm{C}$; $I_{\mathrm{r,t}}$ denotes the radiation intensity during actual operation; α_{T} represents the power temperature coefficient of the PV system; T_{t} is the actual operating temperature of the photovoltaic power supply. In addition, the output curve of the PV system obtained by fitting the irradiance of typical days in all seasons is shown in **Figure 2** (Sara et al., 2020).

Load Timing Model

The load size shows certain regularity due to people's living habits. **Figure 3** shows the typical load curve of residents in all seasons (Velasquez et al., 2016).

Objective Function

Power Losses

The power losses index takes into account the total active power loss of 96 h in four typical days, which is established as follows (Velasquez et al., 2016):

$$\min f_1(x) = \sum_{t=1}^{T} \sum_{i=1}^{n} \sum_{j=1}^{n} A_{ij} \cdot \left(P_i P_j + Q_i Q_j\right) + B_{ij} \cdot \left(Q_i P_j - P_i Q_j\right), \tag{3}$$

$$\begin{cases} A_{ij} = \dfrac{R_{ij} \cdot \cos\left(\delta_i - \delta_j\right)}{V_i V_j} \\ B_{ij} = \dfrac{R_{ij} \cdot \sin\left(\delta_i - \delta_j\right)}{V_i V_j} \end{cases}, \tag{4}$$

where P_i and Q_i are the active power and reactive power injected into node i, respectively; R_{ij} represents the resistance of the transmission line connecting the ith node with the jth node; N means the number of nodes in the distribution network; V_i and δ_i are the voltage and angle of node i, respectively; T is the number of simulation periods; the value is 96.

Voltage Profile

Reasonable access of DG to the distribution network can effectively improve the voltage profile. Therefore, this work adopts the total voltage deviation of 96 h in four typical days to measure the optimization effect, and the voltage profile index is established as follows (Ali and Mohammad, 2021):

$$\min f_2(x) = \sum_{t=1}^{T} \sum_{i=1}^{n} \left(V_{\mathrm{DG},i} - V_{\mathrm{rated}}\right)^2, \tag{5}$$

where $V_{\mathrm{DG},i}$ is the voltage of the ith node after DG is configured in the distribution network and V_{rated} is the rated voltage with a value of 1 p.u.

Pollution Emission

In order to reduce the emission of polluting gases, this work adopts the pollution emission considering carbon dioxide, sulfur dioxide, and nitrogen compounds as follows (Ali and Mohammad, 2021):

$$\begin{aligned} \min f_3(x) = \sum_{t=1}^{T} \sum_{i=1}^{k} P_{\mathrm{DG},i} \cdot \eta_{i,k} \cdot \Big(& ew_{\mathrm{CO_2}} \cdot AE_{pi,\mathrm{co_2}} + ew_{\mathrm{SO_2}} \cdot AE_{pi,\mathrm{so_2}} \\ & + ew_{\mathrm{NO_x}} \cdot AE_{pi,\mathrm{NO_x}} \Big), \end{aligned} \tag{6}$$

where $P_{\mathrm{DG},i}$ is the rated active power output of the ith DG; $\eta_{i,k}$ means the output efficiency of the ith DG at time t; k denotes the number of DG in the distribution network; $AE_{pi,\mathrm{co_2}}$, $AE_{pi,\mathrm{so_2}}$, and $AE_{pi,\mathrm{NO_x}}$ are, respectively, the mass of carbon dioxide, sulfur dioxide, and nitrous oxide released by unit power output of the ith DG. In addition, $ew_{\mathrm{CO_2}}$, $ew_{\mathrm{SO_2}}$, and $ew_{\mathrm{NO_X}}$ are the weight coefficients among different gases, and their values are 0.5, 0.25, and 0.25, respectively.

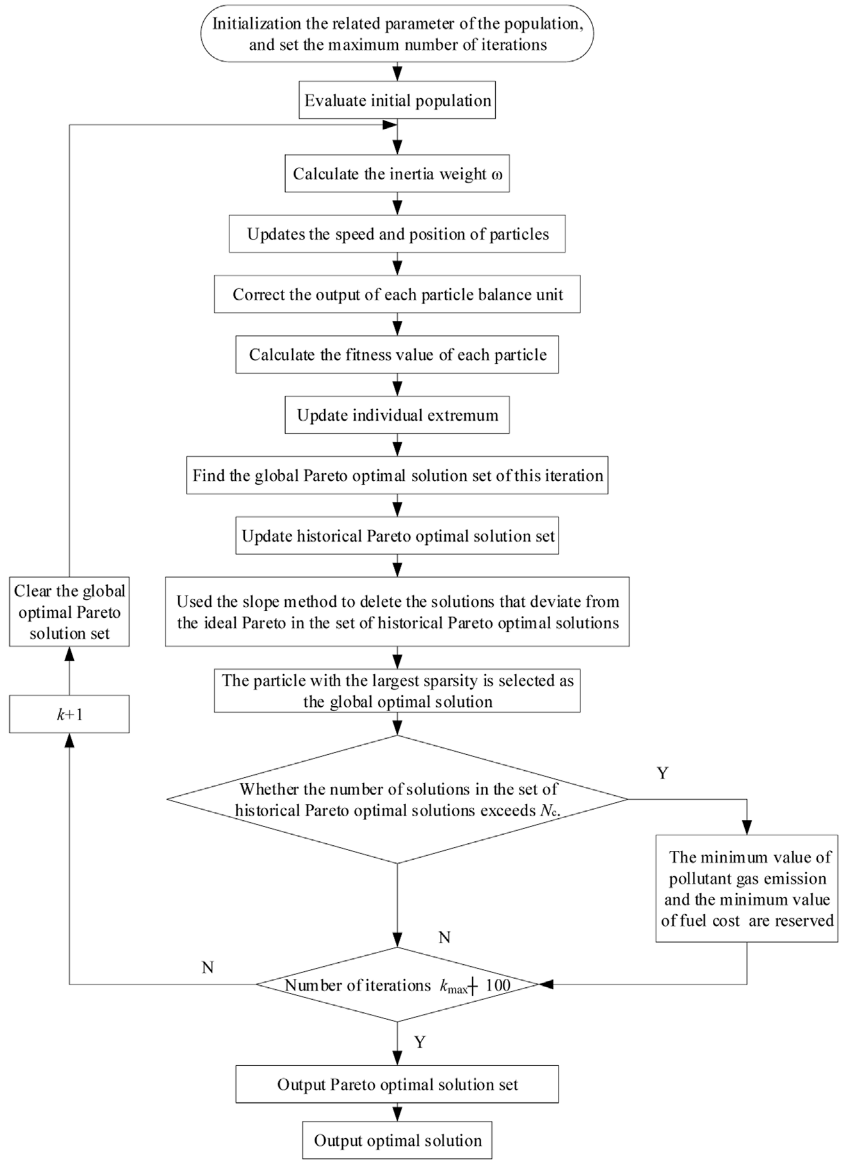

FIGURE 4 | Computational flowchart of the proposed method.

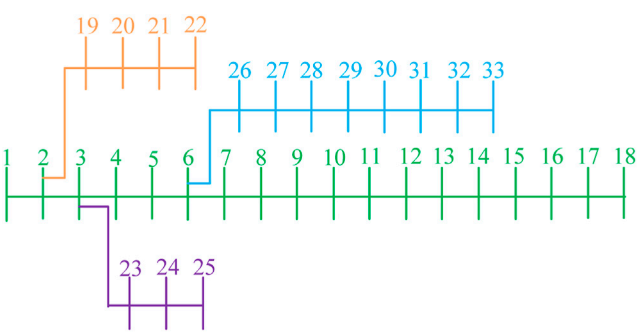

FIGURE 5 | IEEE 33-bus distribution network.

Economic Indicators

The economic cost of DG planning determination includes the investment cost and average operation and maintenance cost of all units, which can be expressed by the following formula (Ali and Mohammad, 2021):

$$\min f_4(x) = \sum_{i=1}^{k} \left(1.3C_{\text{capital},i} \cdot P_{\text{DG},i} + C_{\text{maintenance},i} \cdot P_{\text{DG},i} \cdot t_{\text{operation}}\right), \tag{7}$$

where $C_{\text{capital},i}$ and $C_{\text{maintenance},i}$ are the investment and average operation and maintenance cost of the ith DG, respectively. It is worth noting that $t_{\text{operation}}$ is the running time of DG. The total

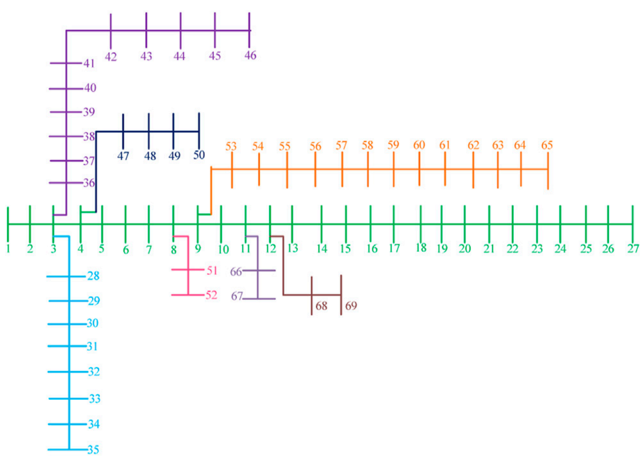

FIGURE 6 | IEEE 69-bus distribution network.

working time of each unit is considered to be 20 years, and the annual working time is 300 days; that is, $t_{\text{operation}}$ = 144,000 h. In addition, the cost and pollution emission statistics of different types of DG are detailed in the literature (Ali and Mohammad, 2021).

Constraints

In order to ensure the safe and stable operation of the system, the following constraints are designed (Bikash et al., 2020; Ali and Mohammad, 2021):

Power Balance Constraints

$$\sum_{i=1}^{n} P_i = \sum_{i=1}^{n} P_{\mathbf{load},i} + P_L - \sum_{i=1}^{n} P_{\mathrm{DG},i}, \tag{8}$$

$$\sum_{i=1}^{n} Q_i = \sum_{i=1}^{n} Q_{\mathbf{load},i} + Q_{\mathrm{L}} - \sum_{i=1}^{n} Q_{\mathrm{DG},i}, \tag{9}$$

where $P_{\mathbf{load},i}$ and $Q_{\mathbf{load},i}$ denote the active and reactive loads at the ith node, respectively; $P_{\mathrm{DG},i}$ and $Q_{\mathrm{DG},i}$ mean the active power and reactive power output by the ith node DG, respectively; P_{L} and Q_{L} are the active power losses and reactive power losses in the distribution network, respectively.

Power Constraints of Transmission Lines

$$S_l \le \left|S_l^{\max}\right|, \tag{10}$$

where S_l is the apparent power flowing through lth line and $S_l^{\max}$ is the maximum apparent power allowed to flow through lth line.

Voltage Constraint

The voltage of the jth node after DG configuration can be calculated by (Abdurrahman et al., 2020)

$$V_{\mathrm{DG},j}^{\min} \le V_{\mathrm{DG},j} \le V_{\mathrm{DG},j}^{\max}, \tag{11}$$

where $V_{\mathrm{DG},j}^{\max}$ and $V_{\mathrm{DG},j}^{\min}$ are the voltage upper and lower limits of the jth node after DG configuration and their values are 1.05 and 0.9, respectively (Suresh and Edward, 2020).

Distributed Power Supply Sizing Constraints

$$P_{\mathrm{DG}}^{\min} \le P_{\mathrm{DG}} \le P_{\mathrm{DG}}^{\max}, \tag{12}$$

$$P_{\mathrm{DG}}^{\min} = 0.1 \sum_{i=1}^{n} P_{\mathbf{load},i}, \tag{13}$$

$$P_{\mathrm{DG}}^{\max} = 0.8 \sum_{i=1}^{n} P_{\mathbf{load},i}, \tag{14}$$

where $P_{\mathrm{DG}}^{\max}$ and $P_{\mathrm{DG}}^{\min}$ are the upper and lower limits of the total active power output of P_{DG}.

MOPSO ALGORITHM

Particle Swarm Optimization Algorithm

Particle swarm optimization is a heuristic algorithm that mimics bird foraging, which can conduct intelligent guidance optimization through cooperation and competition among particles (Doagou-Mojarrad et al., 2013).

Suppose a population has m particles, each particle has an N-dimensional variable, and the position and flight speed of the ith particle in the kth iteration are $X_i^k = [x_{i,1}^k, x_{i,2}^k, \ldots, x_{i,n}^k]$ and $V_i^k = [v_{i,1}^k, v_{i,2}^k, \ldots, v_{i,n}^k]$, respectively. Through evaluating the fitness value of the objective function, the individual optimal position $P_i^k = [p_{i,1}^k, p_{i,2}^k, \ldots, p_{i,n}^k]$ and the population optimal position $G_i^k = [g_{i,1}^k, g_{i,2}^k, \ldots, g_{i,n}^k]$ of each particle are

TABLE 1 | Optimization results of MOPSO.

Generator	Bus location	DG sizing (kVA)	Losseses function (MW)	Voltage function (p.u.)	Emission function (kg)	DG cost (¥)
The first PV	3	649.201	2108.5	53.2049	1.87×10^7	3.45×10^7
The second PV	32	401.55				
The first wind turbine	31	334.646				
The second wind turbine	22	453.685				
Microturbine	8	16.5259				
Fuel cell	9	382.853				

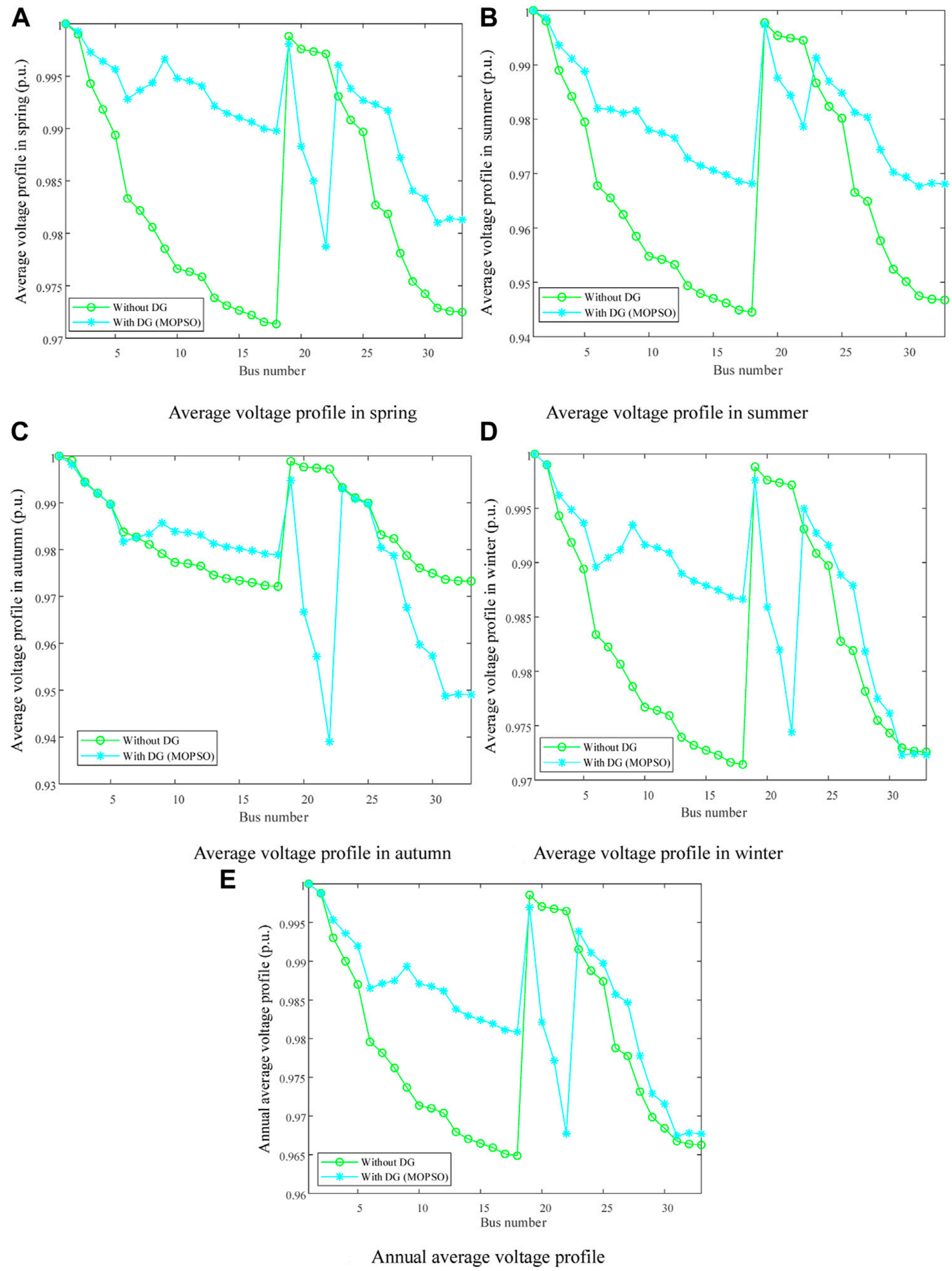

FIGURE 7 | Voltage profile improvement of the IEEE 33-bus distribution network.

determined, and the velocity and position of particle I in the next iteration are determined by (Doagou-Mojarrad et al., 2013)

$$\begin{cases} v_{i,j}^{k+1} = \omega \cdot v_{i,j}^{k} + c_1 r_1 \cdot \left(p_{i,j}^{k} - x_{i,j}^{k}\right) + \\ c_2 r_2 \cdot \left(g_{i,j}^{k} - x_{i,j}^{k}\right) j = 1, 2, \ldots, n \\ x_{i,j}^{k+1} = x_{i,j}^{k} + v_{i,j}^{k+1} \end{cases}, \tag{15}$$

where r_1 and r_2 denote random numbers obeying uniform distribution on the interval (0,1); c_1 and c_2 represent learning factors, both of which are normal numbers. ω is the inertia weight used to balance the global and local optimization capabilities among particles. The value of ω is usually calculated using (Doagou-Mojarrad et al., 2013)

$$w = w_{\max} - \frac{w_{\max} - w_{\min}}{K} k, \tag{16}$$

where K is the maximum number of iterations; k is the current iteration times; $w_{\max} = 0.9$; $w_{\min} = 0.4$.

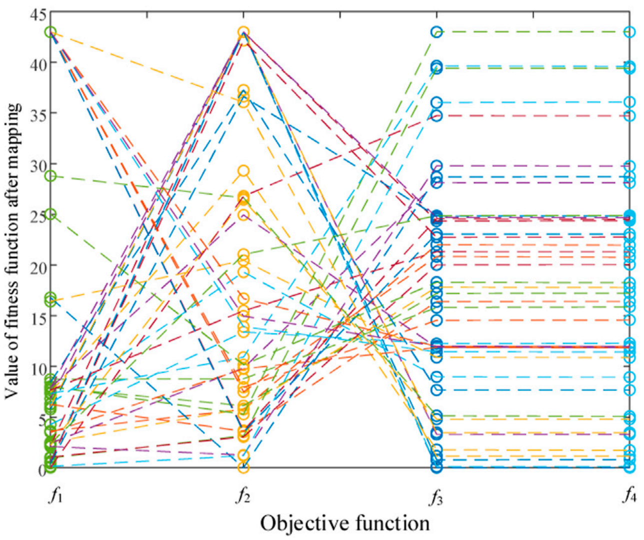

FIGURE 8 | Pareto front results.

MOPSO Algorithm

In order to constantly update a set of Pareto optimal solutions obtained by MOPSO during iterations, this work designs the historical Pareto optimal solution set and the global Pareto optimal solution set during iterations with the help of archiving technology. Global Pareto optimal solution set holds all Pareto optimal solutions generated during the current iteration.

Assuming that a population contains m particles and each particle has N_{obj} objective function value, the global Pareto optimal solution set generated by each iteration is found by the following (Doagou-Mojarrad et al., 2013):

1) Let $i = 1$.
2) Compare particle x_i with particle x_j for all j = 1, 2, . . . , m and $j \neq i$.
3) If j exists so that particle x_j dominates x_i, then particle x_i is marked as the inferior solution.
4) If $i > m$, turn to 5). Otherwise, let $i = i + 1$ and turn to (2).
5) Remove all marked solutions, and the remaining solutions constitute the global Pareto optimal solution set of this iteration.

Historical Pareto optimal solution set: this solution set is used to hold the Pareto optimal solution throughout the iteration. Update the historical Pareto optimal solution set in each iteration: the global Pareto optimal solution set generated in this iteration is merged into the historical Pareto optimal solution set, and noninferior solutions are found according to the Pareto dominant condition, while all inferior solutions are deleted.

With the increase of iteration numbers, the number of solutions in the historical Pareto optimal solution set increases rapidly. To improve the running speed of the algorithm, the number of solutions in the historical Pareto optimal solution set is limited to the present value N_C. When the number of solutions in the historical Pareto optimal solution set exceeds N_C, the sparsity ranking method based on crowding distance is adopted to reduce the number of solutions in the solution set to N_C (Nagaballi and Kale, 2020).

In MOPSO, the individual optimal solution and the global optimal solution of the population need to be redefined. In this work, the individual optimal solution and global optimal solution of MOPSO algorithm are defined as follows.

Individual optimal solution: if the particle generated during this iteration dominates the individual optimal solution of the previous iteration, the individual optimal solution of the particle is updated to the particle generated during this iteration. Otherwise, the individual optimal solution of the particle remains.

Global optimal solution: the global optimal solution is selected from the historical Pareto optimal solution set. According to the sparsity of each particle in the solution set, the particle with the largest sparsity was selected as the global optimal solution of the current iteration.

So far, the filtering mechanism of Pareto is described as follows (Doagou-Mojarrad et al., 2013):

$$k_{i,i+1} = \frac{\left(f_{2,i} - f_{2,i+1}\right)/\left(f_{2,\max} - f_{2,\min}\right)}{\left(f_{1,i} - f_{1,i+1}\right)/\left(f_{1,\max} - f_{1,\min}\right)}, \tag{17}$$

$$k_{i-1,i+1} = \frac{\left(f_{2,i-1} - f_{2,i+1}\right)/\left(f_{2,\max} - f_{2,\min}\right)}{\left(f_{1,i-1} - f_{1,i+1}\right)/\left(f_{1,\max} - f_{1,\min}\right)}, \tag{18}$$

where $k_{i,i+1}$ denotes the normalized slope between the Pareto optimal solution I and its adjacent solution $i + 1$; $k_{i-1,i+1}$ means the normalized slope between the two solutions $i - 1$ and $i + 1$ adjacent to the Pareto optimal solution I. If $k_{i,i+1} > k_{i-1,i+1}$, then the Pareto optimal solution I is close to the ideal Pareto optimal front, and such a solution is retained. If $k_{i,i+1} \leq k_{i-1,i+1}$, it indicates that the Pareto optimal solution i deviates far from the ideal Pareto optimal front, and such a solution is deleted. In addition, the flowchart of MOPSO is given in **Figure 4**(Doagou-Mojarrad et al., 2013).

TABLE 2 | Optimization results of MOPSO.

Generator	Bus location	DG sizing (kVA)	Losseses function (MW)	Voltage function (p.u.)	Emission function (kg)	DG cost (¥)
The first PV	14	217.713	2607.21	47.4124	1.59×10^7	4.12×10^7
The second PV	61	11.3952				
The first wind turbine	26	164.807				
The second wind turbine	12	329.529				
Microturbine	5	326				
Fuel cell	20	49.9061				

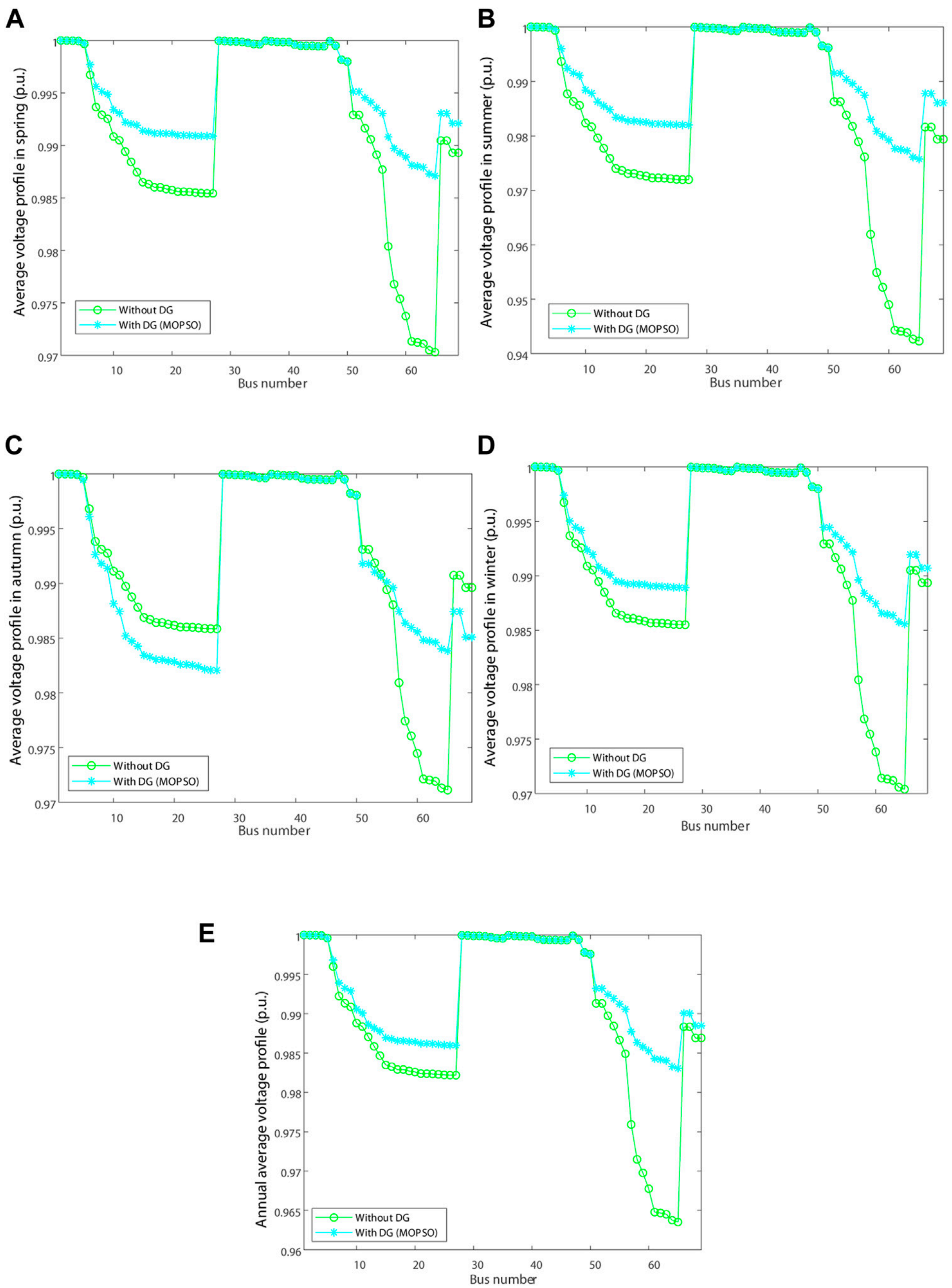

FIGURE 9 | Voltage profile improvement of the IEEE 69-bus distribution network.

CASE STUDIES

As shown in **Figure 5** and **Figure 6**, DG planning research on an IEEE 33-bus and 69-bus distribution network is carried out to verify the effectiveness of the proposed method, including PV system (two nodes installed), wind turbine (two nodes installed), fuel cell (one node installed), and microturbine (one node installed). It is worth noting that fuel cell and micro-gas turbine can carry out power output stably. When PV system and wind turbine are used together, the defect of fluctuating output power can be well compensated. In addition, in four typical days, the total active power loss of the network is 4061.87 kW, while the total voltage deviation is 66.1991 p.u. and the proposed method was coded in MATLAB 2017b.

IEEE 33-Bus Distribution Network

The simulation results obtained by MOPSO and the voltage distribution of the optimized IEEE 33-bus distribution network are shown in **Table 1** and **Figure 7**, respectively. It can be seen from **Table 1** that, after MOPSO optimization,

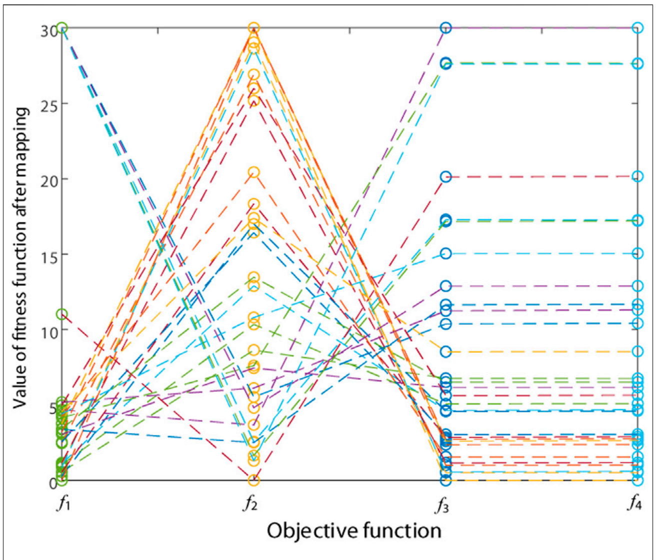

FIGURE 10 | Pareto front results.

the power losses and voltage profile of the distribution network are significantly improved after different types of DG are configured because DG is always installed near the load. It is worth noting that the voltage distribution of the whole system is improved, although the addition of the fan makes the voltage of some nodes deteriorate. In addition, the Pareto front obtained by MOPSO properly distributes the weight of the objective function under the improved ideal point decision method, which effectively carries out the tradeoff optimization of each objective function and avoids the influence brought by the subjective setting of the weight coefficient. Besides, the multiobjective decision-making method described in literature (Zeng and Shu, 2020) is adopted in this work, while the weight coefficients of each objective function obtained are 0.31, 0.15, 0.28, and 0.26, respectively.

In addition, since four different indexes are optimized in this work, Pareto solution set graph cannot be drawn in the Cartesian coordinate system, so the method of mapping the Pareto solution set from the Cartesian coordinate system to a parallel lattice coordinate system is adopted. The Pareto solution set obtained after MOPSO runs 10 times is given in **Figure 8**. Different optimization objectives are mapped to different columns of the parallel lattice coordinate system. In addition, the ordinate represents the fitness function value after mapping, and the dotted line connects the parallel lattice coordinate components of the same objective vector in different columns. In general, MOPSO can show strong searching ability, as well as obtaining widely distributed and uniform Pareto fronts.

IEEE 69-Bus Distribution Network

The optimization results obtained by each algorithm and the voltage distribution of IEEE 69 node distribution network optimized by each algorithm are shown in **Table 2** and **Figure 9**, respectively. It can be seen that, after MOPSO optimization, power loss and voltage distribution of distribution network with different types of DG are significantly improved. Pareto front results are given in **Figure 10**. The weight coefficients of each objective function obtained are 0.28, 0.11, 0.28, and 0.33, respectively.

CONCLUSION

In this work, MOPSO is used to optimize the location and sizing of DG, which contributions are outlined as follows:

1. The objective function with four indexes of distribution network losseses reduction index, voltage profile index, environmental emission reduction index, and economic indicators is established to comprehensively optimize the distribution network.
2. Based on an IEEE 33-bus and 69-bus distribution network, it is effectively verified that MOPSO has strong global searching efficiency and high convergence speed. Also, it can effectively avoid falling into local optimum under complex objective function.
3. Four types of DG, PV station, wind turbine, fuel cell, and microturbine are installed, and the connection of microturbine and fuel cell can stabilize the instability of PV station and wind turbine. The experimental results show that the power losseses of the distribution network optimized by MOPSO decrease by 51.91%, and the voltage profile is also significantly improved.

In future studies, more advanced solution algorithms and multiobjective decision-making method will be devised to solve this problem.

DATA AVAILABILITY STATEMENT

The original contributions presented in the study are included in the article/Supplementary Material; further inquiries can be directed to the corresponding author.

AUTHOR CONTRIBUTIONS

DY: conceptualization and writing—reviewing and editing. JJ: writing—original draft preparation and investigation. WW: writing—reviewing and editing. WC: supervision. DA: supervision. KL: conceptualization and resources. BY: writing—reviewing and editing, software.

FUNDING

This work is supported by the Scientific Research Projects of Inner Mongolia Power (Group) Co., Ltd. (Internal Electric Technology (2021) No. 3).

REFERENCES

Abdurrahman, S., Sun, Y. X., and Wang, Z. H. (2020). Multi-objective for Optimal Placement and Sizing DG Units in Reducing Losses of Power and Enhancing Voltage Profile Using BPSO-SLFA. *Energ. Rep.* 6, 1581–1589. doi:10.1016/j.egyr.2020.06.013

Ali, A., and Mohammad, K. S. (2021). Optimal DG Placement in Power Markets from DG Owners' Perspective Considering the Impact of Transmission Costs. *Electric Power Syst. Res.* 196, 107218. doi:10.1016/j.epsr.2021.107218

Aman, M. M., Jasmon, G. B., Bakar, A. H. A., and Mokhlis, H. (2013). A New Approach for Optimum DG Placement and Sizing Based on Voltage Stability Maximization and Minimization of Power Losses. *Energ. Convers. Management* 70, 202–210. doi:10.1016/j.enconman.2013.02.015

Aman, M. M., Jasmon, G. B., Bakar, A. H. A., and Mokhlis, H. (2014). A New Approach for Optimum Simultaneous Multi-DG Distributed Generation Units Placement and Sizing Based on Maximization of System Loadability Using HPSO (Hybrid Particle Swarm Optimization) Algorithm. *Energy* 66, 202–215. doi:10.1016/j.energy.2013.12.037

Aman, M. M., Jasmon, G. B., Mokhlis, H., and Bakar, A. H. A. (2012). Optimal Placement and Sizing of a DG Based on a New Power Stability index and Line Losses. *Int. J. Electr. Power Energ. Syst.* 43 (1), 1296–1304. doi:10.1016/j.ijepes.2012.05.053

Bikash, D., Mukherjee, V., and Debapriya, D. (2019). Optimum DG Placement for Known Power Injection from Utility/substation by a Novel Zero Bus Load Flow Approach. *Energy* 175 (15), 228–249. doi:10.1016/j.energy.2019.03.034

Bikash, D., Mukherjee, V., and Debapriya, D. (2020). Optimum Placement of Biomass DG Considering Hourly Load Demand. *Energ. Clim. Change* 1, 100004. doi:10.1016/j.egyr.2020.06.013

Chandrasekhar, Y., and Sydulu, M. S. M. (2012). Multiobjective Optimization for Optimal Placement and Size of DG Using Shuffled Frog Leaping Algorithm. *Energ. Proced.* 14, 990–995. doi:10.1016/j.egypro.2011.12.1044

Doagou-Mojarrad, H., Gharehpetian, G. B., Rastegar, H., and Olamaei, J. (2013). Optimal Placement and Sizing of DG (Distributed Generation) Units in Distribution Networks by Novel Hybrid Evolutionary Algorithm. *Energy* 54, 129–138. doi:10.1016/j.energy.2013.01.043

Gopiya Naik, S., Khatod, D. K., and Sharma, M. P. (2013). Optimal Allocation of Combined DG and Capacitor for Real Power Loss Minimization in Distribution Networks. *Int. J. Electr. Power Energ. Syst.* 53, 967–973. doi:10.1016/j.ijepes.2013.06.008

Iqbal, F., Khan, M. T., and Siddiqui, A. S. (2018). Optimal Placement of DG and DSTATCOM for Loss Reduction and Voltage Profile Improvement. *Alexandria Eng. J.* 57 (2), 755–765. doi:10.1016/j.aej.2017.03.002

Kumar, S., Mandal, K. K., and Chakraborty, N. (2019). Optimal DG Placement by Multi-Objective Opposition Based Chaotic Differential Evolution for Techno-Economic Analysis. *Appl. Soft Comput.* 78, 70–83. doi:10.1016/j.asoc.2019.02.013

Li, R. S., Wong, P., Wang, K., Li, B., and Yuan, F. (2020). Power Quality Enhancement and Engineering Application with High Permeability Distributed Photovoltaic Access to Low-Voltage Distribution Networks in Australia. *Prot. Control. Mod. Power Syst.* 5 (3), 1–7. doi:10.1186/s41601-020-00163-x

Mehleri, E. D., Sarimveis, H., Markatos, N. C., and Papageorgiou, L. G. (2012). A Mathematical Programming Approach for Optimal Design of Distributed Energy Systems at the Neighbourhood Level. *Energy* 44 (1), 96–104. doi:10.1016/j.energy.2012.02.009

Murty, V. V. S. N., and Kumar, A. (2015). Optimal Placement of DG in Radial Distribution Systems Based on New Voltage Stability index under Load Growth. *Int. J. Electr. Power Energ. Syst.* 69, 246–256. doi:10.1016/j.ijepes.2014.12.080

Nagaballi, S., and Kale, V. S. (2020). Pareto Optimality and Game Theory Approach for Optimal Deployment of DG in Radial Distribution System to Improve Techno-Economic Benefits. *Appl. Soft Comput.* 92, 106234. doi:10.1016/j.asoc.2020.106234

Nezhadpashaki, M. A., Karbalaei, F., and Abbasi, S. (2020). Optimal Placement and Sizing of Distributed Generation with Small Signal Stability Constraint. *Sustainable Energ. Grids Networks* 23, 100380. doi:10.1016/j.segan.2020.100380

Pabu, P. V., and Singh, S. P. (2016). Optimal Placement of DG in Distribution Network for Power Losses Minimization Using NLP & PLS Technique. *Energ. Proced.* 90, 441–454. doi:10.1016/j.egypro.2016.11.211

Sara, M., Ahmed, E., Tamou, N., and Badr, B. I. (2020). NA Direct Power Control of a DFIG Based-WECS during Symmetrical Voltage Dips. *Prot. Control. Mod. Power Syst.* 5 (1), 36–47. doi:10.1186/s41601-019-0148-y

Satish, K., Vishal, K., and Barjeev, T. (2013). Optimal Placement of Different Type of DG Sources in Distribution Networks. *Int. J. Electr. Power Energ. Syst.* 53, 752–760. doi:10.1016/j.ijepes.2013.05.040

Sultana, U., Khairuddin, A. B., Aman, M. M., Mokhtar, A. S., and Zareen, N. (2016). A Review of Optimum DG Placement Based on Minimization of Power Losses and Voltage Stability Enhancement of Distribution System. *Renew. Sustainable Energ. Rev.* 63, 363–378. doi:10.1016/j.rser.2016.05.056

Surajit, S., and Parimal, A. (2018). Maximization of System Benefits with the Optimal Placement of DG and DSTATCOM Considering Load Variations. *Proced. Computer Sci.* 143, 694–701. doi:10.1016/j.procs.2018.10.446

Suresh, M. C. V., and Edward, J. B. (2020). A Hybrid Algorithm Based Optimal Placement of DG Units for Loss Reduction in the Distribution System. *Appl. Soft Comput.* 91, 106191. doi:10.1016/j.asoc.2020.106191

Velasquez, M. A., Quijano, N., and Cadena, A. I. (2016). Optimal Placement of Switches on DG Enhanced Feeders with Short Circuit Constraints. *Electric Power Syst. Res.* 141, 221–232. doi:10.1016/j.epsr.2016.08.001

Wang, Z., Chen, B., Wang, J., Kim, J., and Begovic, M. M. (2014). Robust Optimization Based Optimal DG Placement in Microgrids. *IEEE Trans. Smart Grid* 5 (5), 2173–2182. doi:10.1109/tsg.2014.2321748

Xi, L., Wu, J., Xu, Y., and Sun, H. (2020). Automatic Generation Control Based on Multiple Neural Networks with Actor-Critic Strategy. *IEEE Trans. Neural Netw. Learn. Syst.* PP (6), 2483–2493. doi:10.1109/TNNLS.2020.3006080

Yan, X. (2020). A Review of Cyber Security Risks of Power Systems: from Static to Dynamic False Data Attacks. *Prot. Control. Mod. Power Syst.* 5 (3), 8–19. doi:10.1186/s41601-020-00164-w

Yang, B., Jiang, L., Wang, L., Yao, W., and Wu, Q. H. (2016). Nonlinear Maximum Power point Tracking Control and Modal Analysis of DFIG Based Wind Turbine. *Int. J. Electr. Power Energ. Syst.* 74, 429–436. doi:10.1016/j.ijepes.2015.07.036

Yang, B., Jiang, L., Yao, W., and Wu, Q. H. (2015). Perturbation Estimation Based Coordinated Adaptive Passive Control for Multimachine Power Systems. *Control. Eng. Pract.* 44, 172–192. doi:10.1016/j.conengprac.2015.07.012

Yang, B., Wang, J., Zhang, X., Yu, T., Yao, W., Shu, H., et al. (2020). Comprehensive Overview of Meta-Heuristic Algorithm Applications on PV Cell Parameter Identification. *Energ. Convers. Management* 208, 112595. doi:10.1016/j.enconman.2020.112595

Yang, B., Yu, T., Shu, H., Zhang, Y., Chen, J., Sang, Y., et al. (2018). Passivity-based Sliding-Mode Control Design for Optimal Power Extraction of a PMSG Based Variable Speed Wind Turbine. *Renew. Energ.* 119, 577–589. doi:10.1016/j.renene.2017.12.047

Yang, B., Yu, T., Zhang, X., Li, H., Shu, H., Sang, Y., et al. (2019). Dynamic Leader Based Collective Intelligence for Maximum Power point Tracking of PV Systems Affected by Partial Shading Condition. *Energ. Convers. Management* 179, 286–303. doi:10.1016/j.enconman.2018.10.074

Yang, B., Zhang, X., Yu, T., Shu, H., and Fang, Z. (2017). Grouped Grey Wolf Optimizer for Maximum Power point Tracking of Doubly-Fed Induction Generator Based Wind Turbine. *Energ. Convers. Management* 133, 427–443. doi:10.1016/j.enconman.2016.10.062

Yang, B., Zhong, L., Zhang, X., Shu, H., Yu, T., Li, H., et al. (2019). Novel Bio-Inspired Memetic Salp Swarm Algorithm and Application to MPPT for PV Systems Considering Partial Shading Condition. *J. Clean. Prod.* 215, 1203–1222. doi:10.1016/j.jclepro.2019.01.150

Zeng, F., and Shu, H. (2020). Memetic Salp Swarm Algorithm-Based Frequency Regulation for Power System with Renewable Energy Integration. *Math. Probl. Eng.* 2020, 1–11. doi:10.1155/2020/6661793

Zhang, K., Zhou, B., Or, S. W., Li, C., Chung, C. Y., and Voropai, N. I. (2021). Optimal Coordinated Control of Multi-Renewable-To-Hydrogen Production System for Hydrogen Fueling Stations. *IEEE Trans. Ind. Applicat.*, 1. doi:10.1109/TIA.2021.3093841

Conflict of Interest: The authors declare that the research was conducted in the absence of any commercial or financial relationships that could be construed as a potential conflict of interest.

Publisher's Note: All claims expressed in this article are solely those of the authors and do not necessarily represent those of their affiliated organizations or those of the publisher, the editors, and the reviewers. Any product that may be evaluated in this article or claim that may be made by its manufacturer is not guaranteed or endorsed by the publisher.